Auris Nasus Larynx 40 (2013) 435–439

Contents lists available at SciVerse ScienceDirect

Auris Nasus Larynx

journal homepage: www.elsevier.com/locate/anl

Long term speech perception after cochlear implant in pediatric patients with *GJB2* mutations

Haruo Yoshida [a,b,*], Haruo Takahashi [b], Yukihiko Kanda [b,c], Shin-ichi Usami [d]

[a] *Department of Otolaryngology-Head and Neck Surgery, National Hospital Organization Ureshino Medical Center, Saga, Japan*
[b] *Department of Otolaryngology-Head and Neck Surgery, Nagasaki University Graduate School of Biomedical Sciences, Nagasaki, Japan*
[c] *Nagasaki Bell Hearing Center, Nagasaki, Japan*
[d] *Department of Otorhinolaryngology, Shinshu University School of Medicine, Asahi, Matsumoto, Japan*

ARTICLE INFO

Article history:
Received 4 September 2012
Accepted 24 January 2013
Available online 9 March 2013

Keywords:
GJB2 hearing impairments
Cochlear implant
Genetic testing
Hereditary hearing loss

ABSTRACT

Objectives: To determine the long term effect of cochlear implant (CI) in children with *GJB2*-related deafness in Japan.
Methods: Genetic testing was performed on 29 children with CI. The speech perception in 9 children with *GJB2* gene-related deafness fitted with CI was compared with those in matched 10 children who were diagnosed as having no genetic loci. The average follow-up period after CI was 55.9 months and 54.6 months, respectively.
Results: A definitive inherited hearing impairment could be confirmed in 12 (41.4%) of the 29 CI children, including 10 with *GJB2*-related hearing impairment and 2 with *SLC26A4*-related hearing impairment. The results of IT-MAIS, word or speech perception testing under the noise, and development of speech perception and production testing using the Enjoji scale were slightly better for the *GJB2* group after CI than for the control group without statistical significant difference.
Conclusion: The long-term results of this study show that CI is also effective in the development of speech performance after CI in Japanese children with *GJB2*-related hearing impairments as HL due to other etiologies.

1. Introduction

Recent progress in the research on hereditary hearing loss is remarkable. Since 1992, more than 125 genetic loci have been reported to be involved in nonsyndromic hearing loss (HL) [1], and over 67 of those loci are involved in autosomal recessive nonsyndromic HL [2]. Among these, the *GJB2* gene encoding the connexin (Cx) 26 protein (chromosomal 13q11-12) is the most common, of which about 100 different *GJB2* mutations have been reported globally [3]. It is reported to account for between 20 and 50% of all recessive nonsyndromic cases [4].

On the other hand, the benefits of cochlear implantation (CI) for spoken language, reading skills, and cognitive development have been clearly demonstrated [5,6]. Recently, the outcomes of CIs in patients with *GJB2* mutations have also been reported. Several studies have shown that patients with *GJB2* mutations (OMIM 121011) usually exhibit excellent speech perception and language performance after CI, when compared with those without identifiable *GJB2* mutations [7–11]. However, other studies have demonstrated that when the control group is appropriately matched with regard to age at implantation and length of post CI, there is no significant difference when comparing those with *GJB2*-related deafness to those without it [12–15]. Results analyzing post-CI speech performance in patients with *GJB2* mutations are still controversial.

In this study, in order to know whether the long term effect of CI is better in children with *GJB2*-related deafness or not, we have studied the speech perception outcome of CI in children with *GJB2* gene mutations, and compared them to those in matched children without inherited hearing loss.

2. Materials and methods

2.1. Subjects

We have performed CI in 301 cases in our clinic since 1997. Genetic testing was performed in 29 children with CI, and definitive *GJB2*- and *SLC26A4*-related hearing impairment was confirmed in 10 (34.5%) and 2 (6.9%) children with CI, respectively.

* Corresponding author at: Department of Otolaryngology-Head and Neck Surgery, Nagasaki University Graduate School of Biomedical Sciences, 1-7-1 Sakamoto, Nagasaki 852-8501, Japan. Tel.: +81 95 849 7349; fax: +81 95 849 7352.
E-mail address: y-haruo@f6.dion.ne.jp (H. Yoshida).

0385-8146/$ – see front matter © 2013 Elsevier Ireland Ltd. All rights reserved.
http://dx.doi.org/10.1016/j.anl.2013.01.006

Table 1
Clinical information of cases in the 2 groups.

Group	Control	GJB2	*P* value
Number of cases	10	9	
Sex (male:female)	3:7	2:7	
Age at CI (months)	36.7	37.4	0.5996
Post CI (months)	54.6	55.9	0.6736
Pre-CI education	Auditory-verbal/oral	Auditory-verbal/oral	

CI: cochlear implantation.

Finally, 19 children whose selection criteria were as follows were enrolled for this study.

1. Their age at CI was 6 years or less
2. Their guardian accepted gene mutation analysis
3. There was no any other apparent cause of deafness such as inner ear anomaly, central disorders/learning difficulties, or cytomegalovirus (CMV) infection

We divided them into two groups: the first, a control group consisting of 10 children who were diagnosed as having no genetic loci, while the second was the actual *GJB2* study group consisting of 9 children with *GJB2* gene-related deafness. Detail of their clinical information is shown in Table 1. HL was diagnosed at a different age in each child, but showed 90 dB or more severe HL before the age of 6 on auditory brainstem response (ABR) test. Preoperative imaging studies (CT and MR) showed no abnormal findings in any of the children in each group. None of the children showed any cognitive delay. The average age at CI in the two groups was 36.7 months (ranging from 21 to 67 months old; 3 male and 7 female) and 37.4 months (ranging from 22 to 63 months old; 2 male and 7 female), respectively. Thus, there is no significant difference between the two groups (Student's *t*-test, $t = -0.5339$, $P = 0.5996$). Their average follow-up period after CI was 54.6 months (ranging from 24 to 110 months) and 55.9 months (ranging from 47 to 62 months), respectively (Student's *t*-test, $t = -0.4278$, $P = 0.6736$). All the cases in this study had an intensive auditory-verbal education without visual information since childhood. Both the CI operation and the (re)habilitation after CI took place in the same clinic.

All patients were fitted with a CI system from either nucleus multichannel cochlear implant system (Cochlear Corporation, Englewood, CO, U.S.A.) or Combi40+ cochlear implant system (MED-EL, Innsbruck, Austria). All electrode arrays were inserted in all patients. There were no perioperative complications in any of the patients.

We examined the hearing level (both with CI and with hearing aids), the Infant-Toddler Meaningful Auditory Integration Scale (IT-MAIS), speech perception skills, and development of articulation in the two groups before and after CI several times in the postoperative period ranging from 6 months to 4 years. The best results from this period were used in evaluating the hearing level and the speech perception skills in the two groups. The speech perception skills were evaluated using CI 2004, SDS-67S, and Japanese CD SDS system (TY-89) tested at 70 dB SPL (sound pressure level) using an open-set questionnaire. We also examined the development of speech perception and production by using the Enjoji Scale of Infant Analytical Development (Enjoji Scale), which was developed in Japan and is now established as one of the standard developmental examinations for evaluating the development of children from birth to about the age of 6 [16]. In this examination, the development of a child can be assessed by checking his or her performance on the chart, in which standard developmental items at each month are described in the three fields including motor, social and language skills. The results allow us to clearly assess to what extent a child is successfully developing in each of the three fields and the six subdivided categories. These tests were conducted up to 2 years after CI.

2.2. Mutation detection

15 ml peripheral venous blood using standard procedure was sent to the Institute of Otorhinolaryngology, Shinshu University School of Medicine, Matsumoto, Japan for Genomic DNA extraction. All subjects underwent mutation screening for 47 common mutations of 10 hearing loss related genes in Japan by using invader assay [17,18].

Written informed consent was obtained from the guardians of all the subjects and the study was approved by the ethical committee of our institute (approval number: 07122106). The differences between in the two groups were analyzed statistically using the paired *t*-test and the unpaired Student's *t*-test. All the acceptance criterion for a significant addition to the explained variance was set at *P* values under 0.05.

3. Results

A definitive *GJB2*-related hearing impairment was confirmed in 9 (32.2%) of the 29 children with CI. Table 2 shows the details of detected *GJB2* gene-mutations. *GJB2* c.235delC was observed in 3 cases, while six children each had one distinct mutation as listed in the table.

Fig. 1 shows the preoperative aided hearing thresholds. The preoperative hearing level was over 90 dB in all the cases, and the average level of preoperative aided hearing thresholds was nearly 60 dB in the two groups presenting no significant difference between the two groups.

Fig. 2 shows the postoperative hearing thresholds with CI. After CI, the hearing level improved to 25–30 dB in both groups, thus there was no significant difference between the groups.

Fig. 3 shows the results of the IT-MAIS for the two groups. Preoperative scores were worse in the *GJB2* group than in the control group, however, these improved from 1 year to 3 years after CI. The averaged IT-MAIS score in the GJB2 group was 9.8 ± 12.9 (range, 0–31) preoperatively. The averaged IT-MAIS score at 2 years after CI increased up to 33.6 ± 7.8 (range, 20–39), and this improvement was statistically significant (paired *t*-test, $P = 0.017$). The averaged IT-MAIS score in the control group at 2 years after CI

Table 2
Mutations with GJB2 gene in 9 cases.

Mutation	Number of cases
GJB2 c.[235delC];[235delC]	3
GJB2 c.[511insAACG];p.[T86R]	1
GJB2 c.[235delC];[299-300delAT]	1
GJB2 p.[G45E;Y136X];[R143W]	1
GJB2 c.[176-191del16];[299-300delAT]	1
GJB2 c.[235delC];p.[G45E;Y136X]	1
GJB2 c.[235delC];p.[R143W]	1

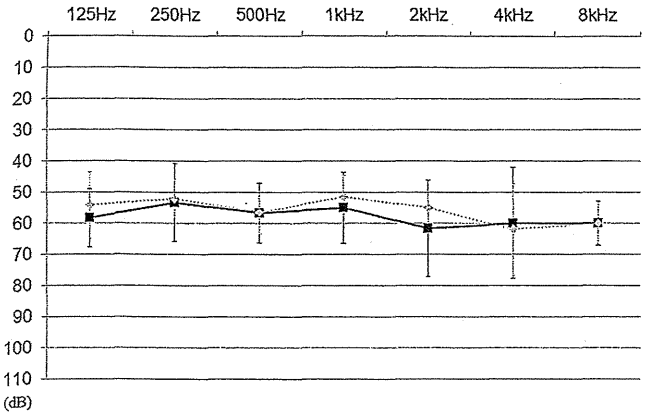

Fig. 1. Results of the average level of preoperative aided hearing thresholds at each frequency. Diamond dots and solid line: control group; square dots and solid line: *GJB2* group; bars: indicate two standard deviations.

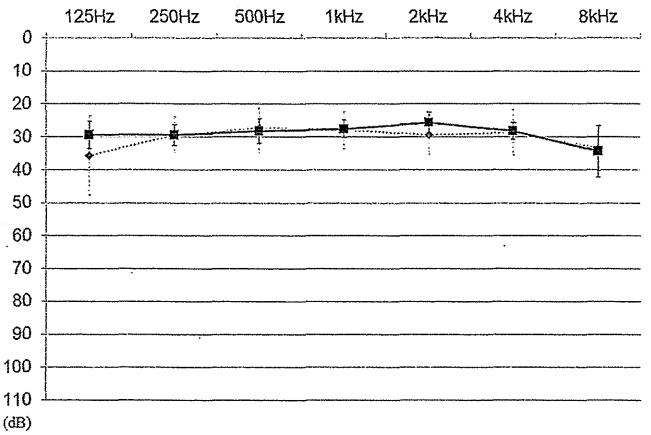

Fig. 2. Results of the average level of postoperative hearing thresholds with CI at each frequency. Diamond dots and solid line: control group; square dots and solid line: *GJB2* group; bars: indicate two standard deviations.

was 30.4 ± 7.6 (range, 19–38). There was no significant difference in the scores between the two groups at 4 years after CI.

Fig. 4 shows the results of speech perception skills in the two groups after CI. Longitudinal axis indicates the results (%) when tested at 70 dB SPL using CI 2004, SDS-67S, and Japanese CD SDS system (TY-89) in the two groups. There was no significant difference between the two groups, but the percentage of correct answers (%) examined under the noise tended to be better in the *GJB2* group.

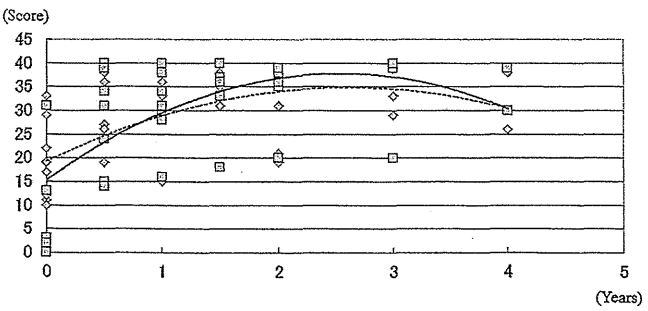

Fig. 3. Results of the difference of IT-MAIS scores from 0 years (=preoperative) to 4 years after CI. Diamond dots: scores in the control group; square dots: scores in the *GJB2* group; dotted line: trend line in the control group; solid line: trend line in the *GJB2* group.

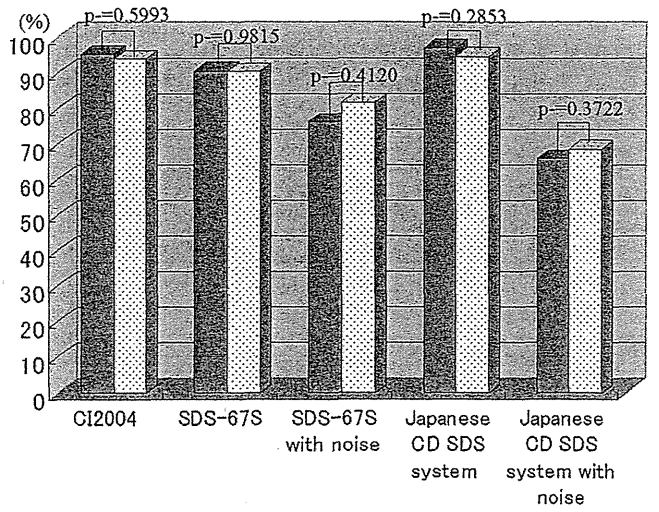

Fig. 4. Results of speech perception skills examined by using CI 2004, SDS-67S, and Japanese CD SDS system (TY-89). Longitudinal axis indicates the correct answer rate (%). Gray bars: control group; dotted bars: *GJB2* group.

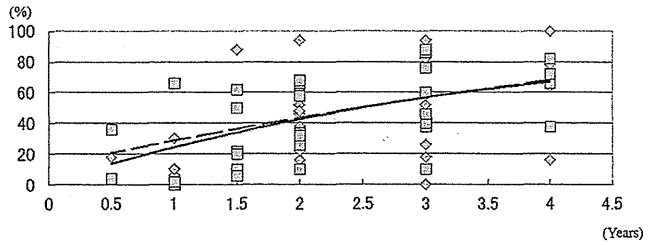

Fig. 5. Results of the development of articulation from 0.5 to 4 years after CI. Diamond dots: accuracy rates in the control group; square dots: accuracy rates in the *GJB2* group.

Fig. 5 shows the results of development of articulation in the two groups after CI. There was no significant difference in the scores between the two groups.

Fig. 6 shows the results in the development of speech perception (Fig. 6a) and production (Fig. 6b) in the two groups after CI. Values of month in the ordinate were calculated by subtracting the developmental months assessed by the Enjoji Scale from the actual age at each period, thus, smaller values indicate better development of speech perception and production. Postoperative language perception and production in the *GJB2* group tended to be slightly better, especially at one and half years after surgery, but there was no significant difference in these scores.

4. Discussion

The incidence of HL is approximately 0.1% among newborns, and hereditary HL is identified in at least 60% of patients with congenital HL, for whom the proportion of syndromic and non-syndromic is 30% and 70%, respectively [19]. The most common trait of nonsyndromic HL is autosomal recessive, which accounts for about 80% of cases [20], and *GJB2* is the gene most frequently associated with hereditary HL. The incidence of *GJB2* mutations in the Japanese population with HL is 14.2% overall and 25.2% in patients with congenital hearing loss [21], and 35 of the 119 cases (29.4%) with non-syndromic deafness [22]. In children with CI, 135 hearing-impaired patients (270 alleles) were tested, and *GJB2* mutations for the c.235delC were found in 39 alleles of 270 alleles (14%). Especially the homozygous of c.235delC was detected in 26

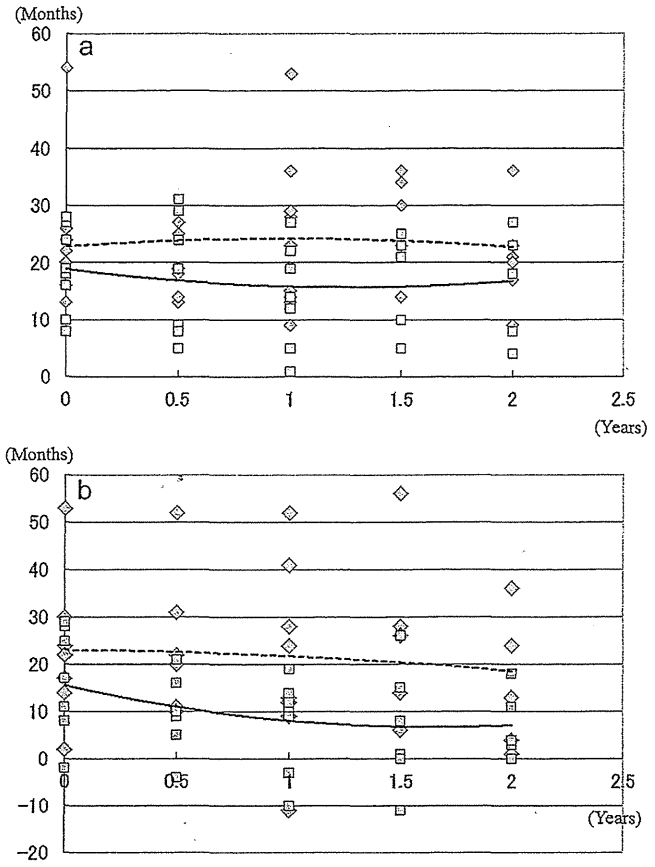

Fig. 6. Results of the developmental course of language perception (a) and production (b) in the control and *GJB2* groups examined by Enjoji Scale of Infant Analytical Development test. Diamond dots: scores in the control group; square dots: scores in the *GJB2* group; dotted line: trend line in the control group; solid line: trend line in the *GJB2* group.

alleles (9.6%), single heterozygous of c.235delC was detected in 1 allele (0.4%) and compound heterozygous of c.235delC was found in 12 alleles (4.4%) [23].

In this study, a definitive inherited hearing impairment could be confirmed in 11 (37.9%) of the 29 CI children, including 9 with *GJB2*-related hearing impairment, 2 with *SLC26A4*-related hearing impairment. These percentages are quite high and remind us of the importance of performing the mutation detection for CI patients.

The *GJB2* group underwent the IT-MAIS, word or speech perception testing under the noise, and development of speech perception and production testing using the Enjoji scale. The finally achieved performances in the two groups were not significantly different, but the averaged IT-MAIS score at 2 years after CI was significantly better in the GJB2 group than in the control group. This result may indicate that the necessary period to achieve the actual age development was shorter in the *GJB2* group than in the control group, and the difference may become smaller as they acquire language through CI in longer term. Matsushiro evaluated 4 CI children with GJB2 gene mutation and reported that the postoperative IT-MAIS score at 6 months was significantly higher in comparison with that of other prelingual CI patients [24]. In this study, children such as those having inner ear anomaly or cytomegalovirus infection, whose postoperative performance after CI is not necessarily good, were excluded from the control group. Considering that these children may also be candidates for CI in general, we can expect CI is efficient for Japanese children with *GJB2* gene mutation as well as for those reported previously [8,23,24].

GJB2 and *GJB6*, mapping to the DFNB1 locus and encoding the gap-junctions Cx 26 and 30, respectively [25]. Cx 26 and 30 are widely expressed in the cochlea at the level of the organ of Corti's supporting cells and connective tissues, and have an important role in forming homomeric or heteromeric hemichannels [26,27]. Mutations in Cx26 are presumed to result in altered potassium recirculation, leading to an accumulation of potassium in the cochlear endolymph and causing hair cell dysfunction and deafness [28]. In other words, mutations in the Cx26 protein mainly lead to the impairment of the endolymph potassium concentrations, which are required for auditory signal transduction, but may not lead to severe damage or decreasing the number of hair cells. It is generally assumed that the results of CI are poorer for inner ear malformation and in cases with neural and/or central damage than in cases with disorders within the inner ear causing the hair cells damage because the auditory pathway including the first neuron, spiral ganglion cells, may well be preserved in the latter. We speculate that the reason why the *GJB2* group had better results in this study is perhaps due to a comparatively good survival and preservation of electrical excitability of the cochlear spiral ganglion cells and the auditory nerve, which is important in the successful CI results [29].

There are some specific reports which support the present results and our speculations. In a rat model, Cx26 was shown to be expressed in nonsensory epithelial and connective tissue cells, but not in the inner or outer hair cells or cochlear nerve fibers [30]. Anatomically, Cx26 mutations result in a dysgenesis of the stria vascularis and hair cells in the organ of Corti, but with minimal neural degeneration and a normal population of spiral ganglion cells in both the apical and basal turns of the cochlea. [31] In the electrophysiological study, children with *GJB2*-related HL had greater similarities between low- and high-frequency residual hearing and between neural activity electrically evoked at apical and basal regions of the cochlea than children with non-*GJB2*-related HL [32]. These results may suggest more consistent spiral ganglion survival along the length of the cochlea in *GJB2*-related HL, which appears to involve a decreasing gradient of spiral ganglion survival from the apex to the base of the cochlea.

Most genotype-phenotype correlation studies have indicated that HL of the subjects with *GJB2* mutations shows a non-progressive pattern [33,34], however, some studies indicated a progressive pattern. [23,35,36]. Considering that early CI is well known to be one of the most important factors for the better postoperative performance for children with congenital HL, even in children with progressive hearing loss due to *GJB2* mutation, we might be able to prepare for early CI for those children if we were aware of it. The early screening of *GJB2* mutation for newborns with severe to profound HL might be advisable.

5. Conclusions

Despite the limits imposed by the small sample size, this study points to the importance of routine genetic assessments. The long-term results of this study also show that CI is also effective in the development of speech performance after CI in Japanese children with *GJB2*-related hearing impairments as HL due to other etiologies. If a child through genetic assessment is diagnosed as having a *GJB2*-related hearing impairment, CI can provide considerable benefits.

Conflict of interest

None.

References

[1] Morell RJ, Kim HJ, Hood LJ, Goforth L, Friderici K, Fisher R, et al. Mutations in the connexin 26 gene (*GJB2*) among Ashkenazi Jews with nonsyndromic recessive deafness. N Engl J Med 1998;339:1500–5.

[2] Van Camp G, Smith RJ. Hereditary hearing loss homepage, http://web-h01.ua.ac.be/hhh/ [accessed 25.01.12].

[3] Xavier E, Paolo G. The Connexin-Deafness homepage, http://davinci.crg.es/deafness/ [accessed 25.01.12].

[4] Denoyelle F, Weil D, Maw MA, Wilcox SA, Lench NJ, Allen-Powell DR, et al. Prelingual deafness: high prevalence of a 30delG mutation in the connexin 26 gene. Hum Mol Genet 1997;6. 2173Y7.

[5] Balkany TJ, Hodges AV, Eshraghi AA, Butts S, Bricker K, Lingvai J, et al. Cochlear implants in children—a review. Acta Otolaryngol 2002;122:356–62.

[6] UK Cochlear Implant Study Group. Criteria of candidacy for unilateral cochlear implantation in postlingually deafened adults. II. Cost-effectiveness analysis. Ear Hear 2004;25:336–60.

[7] Green GE, Scott DA, McDonald JM, Teagle HF, Tomblin BJ, Spencer LJ, et al. Performance of cochlear implant recipients with *GJB2*-related deafness. Am J Med Genet 2012;109:167–70.

[8] Fukushima K, Sugata K, Kasai N, Fukuda S, Nagayasu R, Toida N, et al. Better speech performance in cochlear implant patients with *GJB2*-related deafness. Int J Pediatr Otorhinolaryngol 2002;62:151–7.

[9] Sinnathuray AR, Toner JG, Geddis A, Clarke-Lyttle J, Patterson CC, Hughes AE. Auditory perception and speech discrimination after cochlear implantation in patients with connexin 26 (*GJB2*) gene-related deafness. Otol Neurotol 2004;25:930–4.

[10] Wu CC, Lee YC, Chen PJ, Hsu CJ. Predominance of genetic diagnosis and imaging results as predictors in determining the speech perception performance outcome after cochlear implantation in children. Arch Pediatr Adolesc Med 2008;162:269–76.

[11] Chora JR, Matos TD, Martins JH, Alves MC, Andrade SM, Silva LF, et al. DFNB1-associated deafness in Portuguese cochlear implant users: prevalence and impact on oral outcome. Int J Pediatr Otorhinolaryngol 2010;74:1135–9.

[12] Lustig LR, Lin D, Venick H, Larky J, Yeagle J, Chinnici J, et al. *GJB2* gene mutations in cochlear implant recipients: prevalence and impact on outcome. Arch Otolaryngol Head Neck Surg 2004;130:541–6.

[13] Cullen RD, Buchman CA, Brown CJ, Copeland BJ, Zdanski C, Pillsbury IIIrd HC, et al. Cochlear implantation for children with *GJB2*-related deafness. Laryngoscope 2004;114:1415–9.

[14] Dahl HH, Wake M, Sarant J, Poulakis Z, Siemering K, Blamey P. Language and speech perception outcomes in hearing-impaired children with and without connexin 26 mutations. Audiol Neurootol 2003;8:263–8.

[15] Mesolella M, Tranchino G, Nardone M, Motta S, Galli V. Connexin 26 mutations in nonsyndromic autosomal recessive hearing loss: speech and hearing rehabilitation. Int J Pediatr Otorhinolaryngol 2004;68:995–1005.

[16] Enjoji M, Goya N. Enjoji-shiki Bunsekiteki Kensahou. Tokyo: Keioutusin; 1992.

[17] Abe S, Yamaguchi T, Usami S. Application of deafness diagnostic screening panel based on deafness mutation/gene database using invader assay. Genet Test 2007;11:333–40.

[18] Usami S, Nishio SY, Nagano M, Abe S, Yamaguchi T, Deafness Gene Study Consortium. Simultaneous screening of multiple mutations by invader assay improves molecular diagnosis of hereditary hearing loss: a multicenter study. PLoS One 2012;7:e31276.

[19] Taitelbaum-Swead R, Brownstein Z, Muchnik C, Kishon-Rabin L, Kronenberg J, Megirov L, et al. Connexin-associated deafness and speech perception outcome of cochlear implantation. Arch Otolaryngol Head Neck Surg 2006;132:495–500.

[20] Van Camp G, Willems PJ, Smith RJ. Nonsyndromic hearing impairment: unparalleled heterogeneity. Am J Hum Genet 1997;60:758–64.

[21] Tsukada K, Nishio S, Usami S, Deafness Gene Study Consortium. A large cohort study of *GJB2* mutations in Japanese hearing loss patients. Clin Genet 2010;78:464–70.

[22] Hayashi C, Funayama M, Li Y, Kamiya K, Kawano A, Suzuki M, et al. Prevalence of *GJB2* causing recessive profound non-syndromic deafness in Japanese children. Int J Pediatr Otorhinolaryngol 2011;75:211–4.

[23] Yoshikawa S, Kawano A, Hayashi C, Nishiyama N, Kawaguchi S, Furuse H, et al. The clinical features of patients with the homozygous 235delC and the compound-heterozygous Y136X/G45E of the *GJB2* mutations (Connexin 26) in cochlear implant recipients. Auris Nasus Larynx 2011;38:444–9.

[24] Matsushiro N, Doi K, Fuse Y, Nagai K, Yamamoto K, Iwaki T, et al. Successful cochlear implantation in prelingual profound deafness resulting from the common 233delC mutation of the GJB2 gene in the Japanese. Laryngoscope 2002;112:255–61.

[25] Nance WE. The genetics of deafness. Ment Retard Dev Disabil Res Rev 2003;9:109–19.

[26] Zhao HB, Kikuchi T, Ngezahayo A, White TW. Gap junctions and cochlear homeostasis. J Membr Biol 2006;209:177–86.

[27] Lautermann J, ten Cate WJ, Altenhoff P, Grümmer R, Traub O, Frank H, et al. Expression of the gap-junction connexins 26 and 30 in the rat cochlea. Cell Tissue Res 1998;294:415–20.

[28] Lefebvre PP, Weber T, Rigo JM, Delree P, Leprince P, Moonen G. Potassium-induced release of an endogenous toxic activity for outer hair cells and auditory neurons in the cochlea: a new pathophysiological mechanism in Menière's disease? Hear Res 1990;47:83–93.

[29] Lousteau RJ. Increased spiral ganglion cell survival in electrically stimulated, deafened guinea pig cochleae. Laryngoscope 1987;97:836–42.

[30] Kikuchi T, Kimura RS, Paul DL, Adams JC. Gap junctions in the rat cochlea: immunohistochemical and ultrastructural analysis. Anat Embryol (Berl) 1995;191:101–18.

[31] Jun AI, McGuirt WT, Hinojosa R, Green GE, Fischel-Ghodsian N, Smith RJ. Temporal bone histopathology in connexin 26-related hearing loss. Laryngoscope 2000;110:269–75.

[32] Propst EJ, Papsin BC, Stockley TL, Harrison RV, Gordon KA. Auditory responses in cochlear implant users with and without *GJB2* deafness. Laryngoscope 2006;116:317–27.

[33] Denoyelle F, Marlin S, Weil D, Moatti L, Chauvin P, Garabédian EN, et al. Clinical features of the prevalent form of childhood deafness, DFNB1, due to a connexin-26 gene defect: implications for genetic counselling. Lancet 1999;353:1298–303.

[34] Snoeckx RL, Huygen PL, Feldmann D, Marlin S, Denoyelle F, Waligora J, et al. *GJB2* mutations and degree of hearing loss: a multicenter study. Am J Hum Genet 2005;77:945–57.

[35] Gopalarao D, Kimberling WJ, Jesteadt W, Kelley PM, Beauchaine KL, Cohn ES. Is hearing loss due to mutations in the Connexin 26 gene progressive? Int J Audiol 2008;47:11–20.

[36] Bartsch O, Vatter A, Zechner U, Kohischmidt N, Wetzig C, Baumgart A, et al. *GJB2* mutations and genotype-phenotype correlation in 335 patients from Germany with nonsyndromic sensorineural hearing loss: evidence for additional recessive mutations not detected by current methods. Audiol Neurotol 2010;15:375–82.

Ganaha et al. BMC Medical Genetics 2013, 14:56
http://www.biomedcentral.com/1471-2350/14/56

BMC Medical Genetics

RESEARCH ARTICLE Open Access

Pathogenic substitution of IVS15 + 5G > A in *SLC26A4* in patients of Okinawa Islands with enlarged vestibular aqueduct syndrome or Pendred syndrome

Akira Ganaha[1*†], Tadashi Kaname[2†], Kumiko Yanagi[2†], Kenji Naritomi[2†], Tetsuya Tono[3†], Shin-ichi Usami[4†] and Mikio Suzuki[1†]

Abstract

Background: Pendred syndrome (PS) and nonsyndromic hearing loss associated with enlarged vestibular aqueduct (EVA) are caused by *SLC26A4* mutations. The Okinawa Islands are the southwestern-most islands of the Japanese archipelago. And ancestral differences have been reported between people from Okinawa Island and those from the main islands of Japan. To confirm the ethnic variation of the spectrum of *SLC26A4* mutations, we investigated the frequencies of *SLC26A4* mutations and clinical manifestations of patients with EVA or PS living in the Okinawa Islands.

Methods: We examined 22 patients with EVA or PS from 21 unrelated families in Okinawa Islands. The patient's clinical history, findings of physical and otoscopic examinations, hearing test, and computed tomography (CT) scan of the temporal bones were recorded. To detect mutations, all 21 exons and the exon–intron junctions of *SLC26A4* were sequenced for all subjects. Quantitative reverse-transcription polymerase chain reaction (qRT-PCR) for *SLC26A4* and calculations using the comparative CT ($2^{-\Delta\Delta CT}$) method were used to determine the pathogenicity associated with gene substitutions.

Results: *SLC26A4* mutations were identified in 21 of the 22 patients. We found a compound heterozygous mutation for IVS15 + 5G > A/H723R in nine patients (41%), a homozygous substitution of IVS15 + 5G > A in six patients (27%), and homozygous mutation for H723R in five patients (23%). The most prevalent types of *SLC26A4* alleles were IVS15 + 5G > A and H723R, which both accounted for 15/22 (68%) of the patients. There were no significant correlations between the types of *SLC26A4* mutation and clinical manifestations. Based on qRT-PCR results, expression of *SLC26A4* was not identified in patients with the homozygous substitution of IVS15 + 5G > A.

Conclusions: The substitution of IVS15 + 5G > A in *SLC26A4* was the most common mutation in uniquely found in patients with PS and EVA in Okinawa Islands. This suggested that the spectrum of *SLC26A4* mutation differed from main islands of Japan and other East Asian countries. The substitution of IVS15 + 5G > A leads to a loss of *SLC26A* expression and results in a phenotype of PS and EVA.

* Correspondence: ganahaa@med.u-ryukyu.ac.jp
†Equal contributors
[1]Department of Otorhinolaryngology-Head and Neck Surgery, University of the Ryukyus, Okinawa, Japan
Full list of author information is available at the end of the article

Background

Profound hearing loss affects about 1 in 300 to 1 in 1000 newborns [1-4], and about one-half of these cases can be attributed to genetic factors [5]. About 51% of these cases are due to single nucleotide polymorphisms [5]. As to inheritance pattern among monogenic probands, about 1% is X-linked, 22% is autosomal dominant, and 77% is autosomal recessive [5]. Pendred syndrome (PS) is an autosomal recessive disorder characterized by congenital sensorineural hearing loss and goiter [6]. The causative gene for PS and EVA was identified to be *SLC26A4* [7,8]. Enlarged vestibular aqueduct (EVA) is a common inner ear malformation that can be diagnosed radiographically in patients with impaired hearing (Figure 1). EVA is frequently associated with PS [9-11]. In addition to PS, *SLC26A4* mutations also cause nonsyndromic hearing loss with EVA in the absence of a thyroid phenotype [12,13].

Previous studies revealed that the spectrum of *SLC26A4* mutations varied on the basis of ethnic background [14,15]. Tsukamoto et al. [15] demonstrated that *SLC26A4* mutations occurred in 90% of families with a history of PS and in 78% of families with a history of EVA in Japan. Among these *SLC26A4* mutations, H723R was suggested to have a founder effect in the Japanese population.

The Okinawa Islands are the southwestern-most islands of the Japanese archipelago (Figure 2). Previous studies suggested that there were substantial ancestral differences between Okinawa Islands the main islands of Japan [16]. In this study, we examined patients with EVA or PS from the Okinawa Islands to determine the frequencies and the genotypes of *SLC26A4* mutations and their clinical manifestations.

Methods

Subjects

From May 2008 to July 2012, 22 patients (8 males, 14 females; age range: 0–33 years; mean age: 5.8 years; median age: 8.5 years; Table 1) were diagnosed with PS or EVA in the Department of Otorhinolaryngology, Head and Neck Surgery of the University of the Ryukyus, Japan.

Prior to enrollment, all subjects provided a written informed consent. Our research protocol was approved by the Ethical Review Board of the University of the Ryukyus.

Clinical manifestations of PS and EVA

Clinical history of 22 patients with neuro-otologic symptoms was recorded. A physical examination, including otoscopy, hearing level test, computed tomography (CT) scan of the temporal bones, and examination for thyroid goiter was conducted.

Depending on a subject's ability, hearing level was determined using auditory brainstem response, conditioned orientated response, or pure tone audiogram. Hearing level was defined as the average of the hearing threshold at 0.5, 1.0, 2.0, and 4.0 kHz. Hearing was described as: normal, < 20 dB; mild impairment, 21–40 dB; moderate impairment, 41–70 dB; severe impairment, 71–90 dB; and profound impairment, >91 dB.

Neck palpation or echography of the neck was performed in all patients, to determine thyroid goiter. In addition, their serum levels of thyroid-stimulating hormone (TSH) and free thyroxine (FT4) were measured to evaluate thyroid function (normal values: 0.9–1.6 ng/dl and 0.5–5.0 mU/l, respectively). A perchlorate test was not performed.

High-resolution temporal bone CT was performed in all patients to determine if there were any other inner ear malformations in addition to EVA. EVA was defined as a vestibular aqueduct with a diameter of >1.5 mm at the midpoint between the common crus of the semicircular canal and the external aperture of the vestibular aqueduct on CT [17].

Mondini dysplasia was defined when the cochlea consisted of 1.5 turns in which the middle and apical turns had coalesced to form a cystic apex due to the absence of the interscalar septum [18,19].

Vestibular enlargement was defined when the ratio of the membranous vestibule diameter to the inner ear diameter of the lateral semicircular canal was >1.2 [20].

Vertigo was investigated based on spontaneous nystagmus, caloric vestibular test or patients' self-reporting of past episode. The spontaneous nystagmus was evaluated

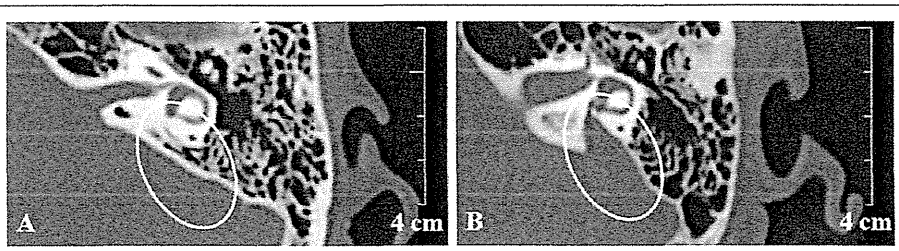

Figure 1 Computed tomography of the temporal bone showing an enlarged vestibular aqueduct. Circles show the vestibular aqueduct. The vestibular aqueduct is not identified in control subject (**A**). The enlarged vestibular aqueduct is identified in a patient with EVA (**B**).

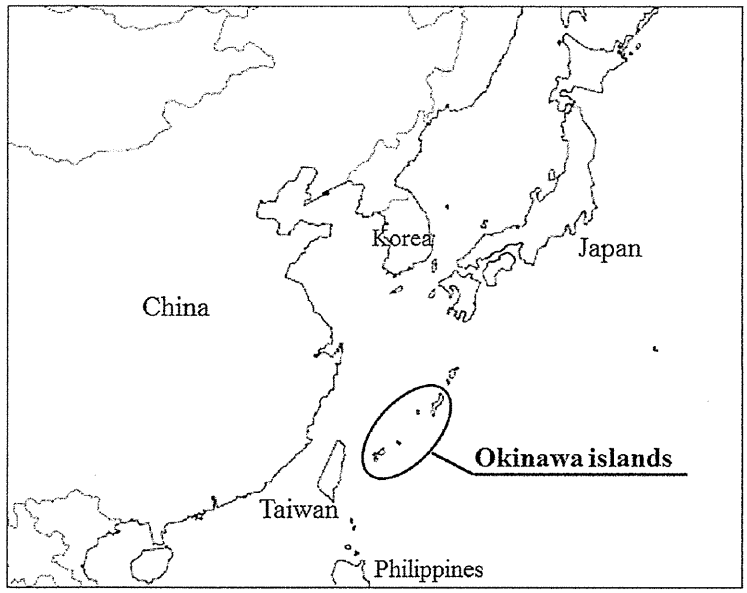

Figure 2 Location of the Okinawa islands in relation to East Asia. The Okinawa islands are located between Taiwan and the Japanese island of Kyushu. The Japanese archipelago comprises Hokkaido, Honshu, Kyusyu, and the Okinawa islands, as well as some smaller islands.

using Frenzel's glass or infrared CCD camera (IRN-1, Morita, Kyoto, Japan).

SLC26A4 genotyping

Genomic DNA was extracted from whole blood using a QIAamp DNA Blood Mini Kit (Qiagen, Hilden, Germany). To detect mutations, all 21 exons and the exon–intron junctions of *SLC26A4* were sequenced for all subjects. A 35 step cycle of Polymerase chain reactions (PCR) was performed as follows: initial denaturation at 94°C for 5 min; 35 cycles of 94°C for 40 s, 60°C for 40 s, and 72°C for 1 min; and a final extension at 72°C for 5 min. PCR reactions were run using a programmable thermal cycler (Verti™ 96-Well Thermal Cycler, Applied Biosystems, CA, USA).

PCR products were purified using a Wizard® SV Gel and PCR Clean-Up System (Promega, WI, USA) and directly sequenced using an ABI PRISM 3130 × l Genetic Analyzer (Applied Biosystems). The sequences obtained were aligned and compared using the BLAST program with known human genome sequences available in the GenBank database.

We surveyed the substitution IVS15 + 5G > A in 100 healthy objects as control.

The genotype of the IVS15 + 5G > A was detected by digestion of the PCR product with the restriction enzyme SspI (New England Biolabs, Ipswich, MA, U.S.A).

Total RNA isolation and reverse-transcription

Total RNA was isolated from leukocytes using a QIAamp RNA Blood Mini Kit (Qiagen) according to the manufacturer's protocol. Before cDNA synthesis, residual DNA was removed by incubation with RNase-free DNase I (Ambion Inc., City, TX, USA). Then, total RNA was reverse transcribed using a TaKaRa Prime Script High Fidelity RT° Kit (TaKaRa, Tokyo, Japan) according to the manufacturer's protocol. Possible contaminating genomic DNA in RNA samples was determined by electrophoresis.

Quantitative nested real-time PCR

Nested real-time quantitative (q) PCR was performed to investigate the level of *SLC26A4* expression in the blood.

First-step PCR (conventional PCR)

A conventional PCR assay was performed in a 10 μl reaction mixture that included 2 μl of cDNA, 0.5 units of DNA Taq polymerase (TaKaRa), 2.5 mM deoxynucleotide triphosphates (dNTPs), 1 μM forward and reverse primers for first-step PCR (Table 2), 10 × buffer, and 1.875 mM $MgCl_2$, with distilled water (H_2O) for the final reaction volume of 10 μl. A 33 step cycle of PCR were performed as follows: 94°C for 5 min, 33 cycles of 94°C for 30 s, 60°C for 30 s, 72°C for 40 s, and a final extension at 72°C for 5 min.

Second-step PCR (quantitative nested PCR)

Following the first PCR, a second PCR was performed using a set of internal primers (Table 2). The reaction mixture contained 1 μl of the first PCR product (diluted 10-fold), 10 μl of SYBR Premix Ex Taq, and 0.2 μM of the internal forward and reverse primers; the final

Table 1 Summary of clinical features of 22 patients

	Age (years)		CT			PTA		Vertigo	Thyroid	
			EVA	MD	VE	HL (dB)	Conductive hearing loss		Goiter	Thyroid function
1	3	R	+	+	+	SO	unknown	-	-	normal
		L	+	+	+	SO	unknown			
2	14	R	+	+	-	105	+	-	+	normal
		L	+	+	-	96	+			
3	21	R	+	+	+	73	+	+	+	normal
		L	+	+	+	91	+			
4	21	R	+	-	-	81	+	+	+	normal
		L	+	-	-	85	+			
5	28	R	+	+	+	96	+	+	+	normal
		L	+	+	+	SO	+			
6	33	R	+	+	-	101	+	+	+	normal
		L	+	+	+	106	+			
7	1	R	+	+	-	SO	unknown	-	-	normal
		L	+	+	+	SO	unknown			
8	1	R	+	-	-	SO	unknown	-	-	normal
		L	+	-	-	103	unknown			
9	2	R	+	+	-	101	unknown	-	-	normal
		L	+	+	-	100	unknown			
10	12	R	+	-	-	95	+	-	+	normal
		L	+	-	-	100	+			
11	29	R	+	+	+	85	+	-	-	
		L	+	+	+	110	+			
12	0	R	+	-	-	55	unknown	+	-	normal
		L	+	-	-	73	unknown			
13	3	R	+	-	+	85	unknown	+	-	normal
		L	+	+	+	58	+			
14	5	R	+	+	+	95	+	+	-	normal
		L	+	+	+	93	+			
15	5	R	+	+	+	103	+	-	-	normal
		L	+	+	+	100	unknown			
16	6	R	+	-	-	81	+	+	-	normal
		L	+	-	-	91	+			
17	7	R	+	-	-	83	+	-	-	normal
		L	+	-	+	81	+			
18	14	R	+	+	+	96	+	-	+	normal
		L	+	+	+	91	+			
19	16	R	+	-	+	91	+	-	+	normal
		L	-	-	+	21	-			
20	26	R	+	-	-	98	+	+	-	normal
		L	+	-	+	103	+			
21	5	R	+	+	+	85	+	-	-	normal
		L	+	+	-	97	+			
22	10	R	+	-	-	53	+	-	-	normal
		L	-	-	-	15	-			

EVA enlarged vestibular aqueduct, *MD* Mondini malformation, *VE* vestibular enlargement, *PTA* pure tone audiogram, *HL* hearing level, *SO* scale out, *NA* no available data.

Table 2 Primer sequences used for nested real-time PCR

Nested PCR assay			Sequence	PCR product size (bp)
First-step PCR (external primer)	Exon 14	forward	TCTTGGAATGGCCTTGGAAGC	282
	Exon 17	reverse	TGAAACAGCATCACTTATGATGC	
Second-step PCR (internal primer)	Exon 15	forward	TGAAGAACCTCAAGGAGTGAAG	154
	Exon 16	reverse	TTTCTGTATTTTCCTCAGCGCT	

reaction volume was adjusted to 20 μl with distilled H_2O. A Light Cycler real-time quantitative PCR system (Roche, Basel Switzerland) was used for amplification and detection of the PCR products. A 40 step cycle of thermal cycler program was performed as follows: denaturation at 95°C for 5 min; 40 cycles of 95°C for 10 s, 60°C for 20 s, and 72°C for 40 s; followed by recording the fluorescence values after each elongation step and melting curve analysis with denaturation at 95°C for 5 s, annealing at 65°C for 1 min, and redenaturation by increasing the temperature to 95°C. The second-step PCR products were separated by 1.5% agarose gel electrophoresis, stained with ethidium bromide, and visualized by UV transillumination. For this analysis, we used three control subjects with no mutations (wild type), three patients compound heterozygous for IVS15 + 5G > A/H723R, and three patients homozygous for IVS15 + 5G > A.

Validation of comparative CT ($2^{-\Delta\Delta CT}$) method and calculations for quantifying *SLC26A4* mRNA

We used the CT ($2^{-\Delta\Delta CT}$) method by assuming approximately equal amplification efficiencies for both target and reference genes. This prerequisite was verified by performing a validation experiment using both *SLC26A4* and a housekeeping gene. Calculations were made using the comparative CT ($2^{-\Delta\Delta CT}$) method. *GAPDH* (glyceraldehyde 3-phosphate dehydrogenase), *PGK-1* (phosphoglycerate kinase 1), and *ACTB* (actin beta) were used as internal reference genes for PCR normalization with regard to the amount of RNA added to the reverse transcription reactions. Normalized results were expressed as the mean ratio of *SLC26A4* mRNA to *GAPDH* mRNA, *PGK-1* mRNA, and *ACTB* mRNA. To evaluate relative transcript levels, the threshold cycle value (Ct) of each sample was used to calculate and compare the ΔCt of each sample to that of the control subject and patients with a compound heterozygous for IVS15 + 5G > A/H723R, and a homozygous for IVS15 + 5G > A. ΔΔCT was also calculated to compare the transcript levels in the control subject, and patients with a compound heterozygous for IVS15 + 5G > A/H723R, and a homozygous for IVS15 + 5G > A. The transcript levels were calculated in each genotype with three subjects and each subject was calculated in triplicate.

Results

Mutation analysis for *SLC26A4*

By direct DNA sequence analysis, *SLC26A4* mutations were observed in 21 of 22 patients. Among the 21 patients with mutations, a compound heterozygous mutation for IVS15 + 5G > A/H723R was identified in nine patients (Figure 3C, D), a homozygous mutation for H723R was identified in five patients (Figure 3E), and a homozygous substitution of IVS15 + 5G > A was identified in six patients (Figure 3F). A compound heterozygous substitutions for IVS15 + 5G > A/T527P was identified in one subject. We could not identify any *SLC26A4* mutations in one subject (Table 3). We could not find the substitution IVS15 + 5G > A in 100 control objects.

Clinical characteristics

Table 1 summarizes the clinical characteristics of all 22 subjects. High-resolution temporal bone CT scans revealed that bilateral EVA was present in 20 patients and unilateral EVA was present in other two. Mondini dysplasia and vestibular enlargement was observed in 17 ears (17/44; 39%) and 22 ears (22/44; 50%), respectively.

Hearing loss grades in the affected ears ranged from moderate to profound in the patients with EVA (Table 1). The hearing levels of the two unaffected ears were normal and mild hearing loss, respectively. Table 4 shows the hearing level distributions based on genotypes. No significant differences were expected in the distributions for hearing level among the five genotype groups due to the small sample of only 22 patients.

Neck examinations revealed thyroid goiters in 8 of 22 patients. Overall, 0% (0/11) and 73% (8/11) of the patients younger and older than 10 years of age, respectively, had a thyroid goiter. Their serum FT4 and TSH levels were within the normal ranges. There is no relation between occurrence of goiter and mutation genotypes.

SLC26A4 expression in patients with IVS15 + 5G > A

Electrophoretic separation of the real-time PCR products did not exhibit any bands in patients with the homozygous substitution for IVS15 + 5G > A (Figure 4C).

Because the *SLC26A4* expression levels were not high in blood samples, we investigated its expression using nested real-time qPCR for three control subjects, three

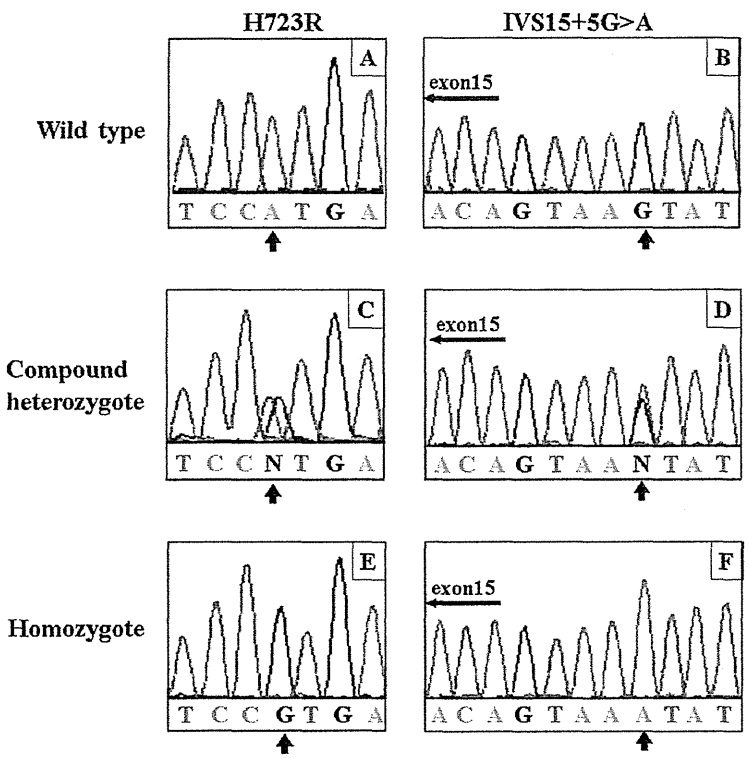

Figure 3 Examples of direct sequence analysis of the *SLC26A4* gene. Representative results of H723R and the IVS15 + 5G > A mutation analysis are shown. Genomic sequences of the *SLC26A4* gene in normal individuals (**A**), (**B**). A compound heterozygous mutation for IVS15 + 5G > A/H723R (**C**), (**D**). A homozygous mutation for H723R (**E**). A homozygous substitution of IVS15 + 5G > A (**F**). The arrows indicate the variant nucleotide.

patients with the compound heterozygous mutation for IVS15 + 5G > A/H723R, and three patients with the homozygous substitution for IVS15 + 5G > A. The control subjects had normal hearing without any malformations of the inner or middle ear and no family history of hearing loss. After obtaining a written informed consent, blood samples were collected from each subject and were subjected to Real-time PCR with SYBR Green and the expression level was evaluated using the comparative CT ($2^{-\Delta\Delta CT}$) method. The relative *SLC26A4* expression levels in the control no.1, control no.2 and control no.3 with no *SLC26A4* mutations were 9089 ± 441.5 (standard deviation), 2417 ± 189.5, and 4956 ± 260.4 respectively. In patient no.12, patient no.14 and patient no.16 with a compound heterozygous mutation for IVS15 + 5G > A/H723R were 979.5 ± 79.12, 2846 ± 206.5 and 1183 ± 33.93 respectively. In patient no.1, patient no.2 and patient no.4 with a homozygous substitution for IVS15 + 5G > A were $1.96 \times 10^{-4} \pm 7.66 \times 10^{-5}$, $5.76 \times 10^{-5} \pm 3.37 \times 10^{-6}$ and $4.35 \times 10^{-5} \pm 8.09 \times 10^{-6}$ respectively (Figure 5).

Based on the results of both electrophoresis and RT-nested qPCR, no *SLC26A4* expression was observed in patients with homozygous substitution of IVS15 + 5G > A.

Discussion

Correlations between *SLC26A4* genotypes and hearing phenotypes

Hearing loss in patients with EVA and PS is usually apparent at the pre- or perilingual stage [6,21]. Hearing loss in EVA and PS is sensorineural with some mixed hearing loss in the low-frequency range [22-27]. The hearing level sometimes deteriorates suddenly and may be followed by a partial recovery, such as with fluctuating hearing loss [28,29]. In our study, hearing loss was detected at the pre- or perilingual stage in all cases except for two cases of unilateral EVA. However, in all cases, hearing levels eventually deteriorated to severe or profound loss (Table 1) and were permanent with or without hearing fluctuation or stepwise hearing deterioration. No significant differences were observed in the hearing levels among the five genotypes (Table 4).

Correlations between *SLC26A4* genotypes and thyroid phenotype

SLC26A4 encodes for the 86 kDa transmembrane protein pendrin [7,30]. In the thyroid, this protein acts as co-transporter of chloride and iodine in the thyroid

Table 3 Distribution of *SLC26A4* genotypes of 22 patients

	Age at onset of hearing loss (years)	Age at genetic test (years)	Sex	Allele 1	Allele 2
1	0	3	M	IVS15 + 5G > A	IVS15 + 5G > A
2	2	14	F	IVS15 + 5G > A	IVS15 + 5G > A
3	3	21	F	IVS15 + 5G > A	IVS15 + 5G > A
4	2	22	F	IVS15 + 5G > A	IVS15 + 5G > A
5	0	23	M	IVS15 + 5G > A	IVS15 + 5G > A
6	0	29	F	IVS15 + 5G > A	IVS15 + 5G > A
7	0	1	F	H723R	H723R
8	1	1	F	H723R	H723R
9	4	2	M	H723R	H723R
10	0	12	F	H723R	H723R
11	5	29	M	H723R	H723R
12	0	0	M	IVS15 + 5G > A	H723R
13	2	3	M	IVS15 + 5G > A	H723R
14	0	5	F	IVS15 + 5G > A	H723R
15	1	5	F	IVS15 + 5G > A	H723R
16	0	6	F	IVS15 + 5G > A	H723R
17	2	7	F	IVS15 + 5G > A	H723R
18	2	14	F	IVS15 + 5G > A	H723R
19	7	16	F	IVS15 + 5G > A	H723R
20	5	26	M	IVS15 + 5G > A	H723R
21	1	5	M	H723R	TS27P
22	7	10	F	ND	ND

ND not determined.

[31,32]. In PS patients, a mutation in *SLC26A4* results in reduced pendrin-induced chloride and iodide transport and, ultimately, goiter [33].

Goiter usually develops around the end of the first decade of life or during young adulthood, although the time of onset and severity vary considerably among patients [12,34], and even within families [35]. Despite an impaired incorporation of iodide, most patients with PS are clinically and biochemically euthyroid [21,34,36].

To our knowledge, no previous studies have investigated correlations between *SLC26A4* genotypes and the thyroid phenotype. In the present study, PS was diagnosed in 8 of 11 patients older than 10 years of age, but not in any of the 11 patients who were younger than 10 years of age. This indicates that it is difficult to diagnose PS before the age of 10 years.

Thyroid function was normal in all of the 21 patients we examined, as demonstrated by their normal serum concentrations of FT4 and TSH. There were no significant differences in serologic thyroid test results and goiter status among patients with homozygous substitution for IVS15 + 5G > A, the H723R homozygous mutation, or compound heterozygous mutation for IVS15 + 5G > A/H723R. Therefore, our results indicate that serologic testing of FT4 and TSH levels is not useful to distinguish between individuals with PS or EVA.

Distributions of *SLC26A4* mutations in EVA and PS patients in Okinawa Islands

It was previously reported that the spectrum of *SLC26A4* mutations varied based on ethnic background [35,36]. H723R and IVS7-2A > G are prevalent alleles that account for the majority of the observed *SLC26A4* mutations in East Asian populations [35]. In the Japanese population, H723R was the most common mutation [15,36,37]. In Chinese and Taiwanese populations, IVS7-2A > G was the most common mutation [38-40], whereas in the Korean population, H723R and IVS7-2A > G were the most frequent and accounted for 60.2% (47/78) and 30.7% (24/78) of the mutated alleles, respectively [41].

Ancestral differences have been reported between people from Okinawa Islands and those from the main islands of Japan based on single-nucleotide polymorphism genotypes [16]. We analyzed *SLC26A4* mutations among 22 patients with EVA or PS from 21 unrelated families. H723R have been reported as the most common mutation found in the main islands of Japan. As with H723R mutation, IVS15 + 5G > A substitution was

Table 4 Clinical features in different genotype groups

Genotype	Hearing level					CT		Vertigo
	Normal	Mild	Moderate	Severe	Profound	MD	VE	
IVS15 + 5 G > A homozygous (n = 6)	0	0	0	3	9	6/12	6/12	4/6
H723R homozygous (n = 5)	0	0	0	1	9	4/10	3/10	0/5
IVS15 + 5 G > A/H723R (n = 9)	0	1	2	4	11	5/18	11/18	4/9
IVS15 + 5G > /T527P (n = 1)	0	0	0	1	1	2/2	1/2	0/1
No mutation (n = 1)	1	0	1	0	0	0/2	0/2	0/1
Subtotal	1	1	3	9	30	17/44	21/44	8/22
Total			44					

Normal: ≤20 dB; Mild: 21–40 dB; Moderate: 41–70 dB; Severe: 71–90 dB; Profound: >91 dB.
MD Mondini malformation, *VE* Vestibular enlargement, *CT* computed tomography.

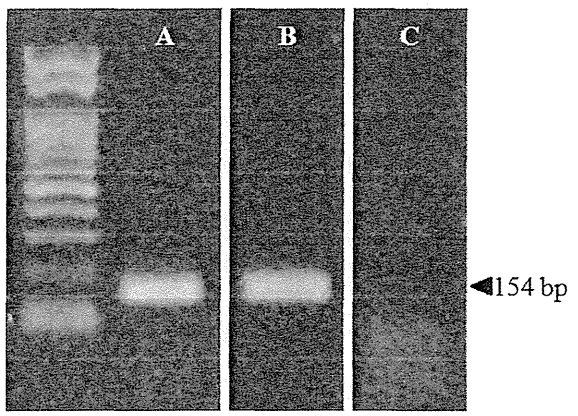

Figure 4 Expression of the *SLC26A4* gene in patients with PS or EVA. The expected RT-nested PCR amplification product of *SLC26A4* was 154 base pairs (bp) in length. Agarose gel electrophoresis shows the 154 bp band for the control subject (**A**) and the patient with IVS15 + 5G > A/H723R compound heterozygous mutation (**B**); however, there was no band for the patient with IVS15 + 5G > A homozygous substitution (**C**).

also identified most frequently in 15 of 22 of our Okinawa patients. The substitution of IVS15 + 5G > A in one allele have been reported only 10 cases in Asian populations [36,42-45]. Thus, IVS15 + 5G > A was the characteristic *SLC26A4* gene mutation among patients in Okinawa Islands, indicating a difference in the spectrum of *SLC26A4* mutations among patients in Okinawa Islands compared with patients in other

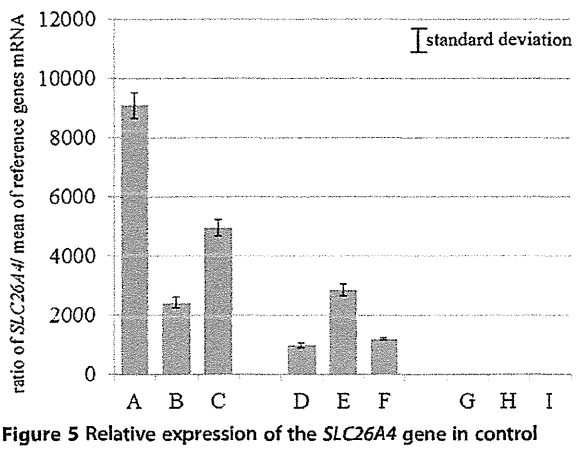

Figure 5 Relative expression of the *SLC26A4* gene in control subjects and in patients with a homozygous mutation of IVS15 + 5G > A or compound heterozygous mutation of IVS15 + 5G > A/H723R. The ratio of SLC26A4 mRNA to GAPDH mRNA is shown in three control subjects (**A, B, C**), three patients with compound heterozygous mutation of IVS15 + 5G > A/H723R (**D, E, F**), and three patients with IVS15 + 5G > A homozygous substitution (**G, H, I**). No expression of *SLC26A4* was observed in the three patients with the IVS15 + 5G > A homozygous substitution (**G, H, I**). All experiments were done in tripricate.

populations. These results suggest that this *SLC26A4* mutation may have originated from a common ancestor.

Pathogenic effect of IVS15 + 5G > A substitution

The heterozygous substitution of IVS15 + 5G > A has been assumed to cause aberrant splicing [36,42-45]. However, Yang et al. [42] could not find any abnormal RT-PCR products related to the size for SLC26A4 sequence analysis in patients with splice mutation. Because its pathogenicity was only implicated on the basis of uncommon polymorphisms, the pathogenic potential of IVS15 + 5G > A still remains unknown.

Substitutions near the canonical splice sites are difficult to classify as pathogenic or non-disease causing. Because such substitutions affect proper RNA splicing but some substitutions do not cause any effect [46-48]. Thus, it is important to determine the pathogenic effect of a particular substitution near the donor site by mRNA analysis [48]. We investigated *SLC26A4* expression in patients with compound heterozygous mutation for IVS15 + 5G > A/H723R and homozygous substitution for IVS15 + 5G > A by RT-PCR and RT-real time PCR by targeting genes around these mutations. No aberrant PCR products were detected in the patient with heterozygous substitution of IVS15 + 5G > A (Figure 4B), which suggests that IVS15 + 5G > A does not cause aberrant splicing, as also argued by Yang et al. However, in patients with the homozygous substitution of IVS15 + 5G > A, *SLC26A4* was not expressed, as shown in Figure 4. In addition, for patients with the heterozygous substitution, *SLC26A4* expression was reduced from the normal control level. These findings suggest that IVS15 + 5G > A disrupts pre-mRNA splicing and causes the loss of *SLC26A4* expression. The patients in Yang et al. [42] were heterozyote so that Yang et al. [42] most likely amplified the non-mutated allele. Taken together, our results indicate that the substitution of IVS15 + 5G > A is a loss-of-function mutation caused by a loss of *SLC26A4* expression.

Conclusions

We found no correlations between the type of *SLC26A4* mutation and hearing levels or the thyroid phenotype. Moreover, thyroid testing using serum FT4 and TSH levels was not useful for distinguishing between individuals with PS and EVA.

The substitution of IVS15 + 5G > A in the *SLC26A4* was unique and the most common in PS and EVA patients from Okinawa Islands. This supports that the spectrum of *SLC26A4* mutations differs by geographic area in East Asia. Our qPCR results for *SLC26A4* indicate that the substitution of IVS15 + 5G > A should be a pathogenic mutation that leads to a loss of *SLC26A4* expression and results in a phenotype of PS and EVA.

Competing interests
The authors declare that they have no competing interests.

Authors' contributions
AG diagnosed the patients, collected clinical data, performed the experiments, and wrote the manuscript. TK, KY, and SU carried out data analysis. KN, TT, and MS edited the manuscript and supervised the project. All authors read and approved the final manuscript.

Acknowledgements
This work was supported in part by the Japan Society for the Promotion of Science (JSPS) KAKENHI Grant-in-Aid for Young Scientists (B) Number 23791914, by Special Account Budget for Education and Research from the Japan Ministry of Education and by research grants from the Japan Ministry of Health, Labor, and Welfare.

Author details
[1]Department of Otorhinolaryngology-Head and Neck Surgery, University of the Ryukyus, Okinawa, Japan. [2]Department of Medical Genetics, University of the Ryukyus, Okinawa, Japan. [3]Department of Otorhinolaryngology-Head and Neck Surgery, University of Miyazaki, Miyazaki, Japan. [4]Department of Otorhinolaryngology, Shinshu University School of Medicine, Nagano, Japan.

Received: 18 January 2013 Accepted: 17 May 2013
Published: 24 May 2013

References

1. Downs MP: **Universal newborn hearing screening–the Colorado story.** *Int J Pediatr Otorhinolaryngol* 1995, **32**:257–259.
2. Mehl AL, Thomson V: **Newborn hearing screening: the great omission.** *Pediatrics* 1998, **101**:E4.
3. Mehl AL, Thomson V: **The Colorado newborn hearing screening project, 1992–1999: on the threshold of effective population-based universal newborn hearing screening.** *Pediatrics* 2002, **109**:E7.
4. Bitner-Glindzicz M: **Hereditary deafness and phenotyping in humans.** *Br Med Bull* 2002, **63**:73–94.
5. Morton NE: **Genetic epidemiogy of hearing impairment.** *Ann NY Acad Sci* 1991, **630**:16–31.
6. Pendred V: **Deaf-mutation and goiter.** *Lancet* 1896, **2**:532.
7. Everett L, Glaser B, Beck J, Idol J, Buchs A, Heyman M, Adawi F, Hazani E, Nassir E, Baxevanis A, Sheffield V, Green E: **Pendred syndrome is caused by mutations in a putative sulphate transporter gene (*PDS*).** *Nat Genet* 1997, **17**:411–422.
8. Li XC, Everett LA, Lalwani AK, Desmukh D, Friedman TB, Green ED, Wilcox ER: **A mutation in PDS causes non-syndromic recessive deafness.** *Nat Genet* 1998, **18**:215–217.
9. Johnsen T, Jørgensen MB, Johnsen S: **Mondini cochlea in Pendred's syndrome.** *Acta Otolaryngol* 1986, **102**:239–247.
10. Nakagawa O, Ito S, Hanyu O, Yamazaki M, Urushiyama M: **Female siblings with Pendred's syndrome.** *Int Med* 1994, **33**:369–372.
11. Reardon W, Trembath RC: **Pendred syndrome - 100 years of underascertainment?** *Q J Med* 1997, **90**:443–447.
12. Campbell C, Cucci RA, Prasad S, Green GE, Edeal JB, Galer CE, Karniski LP, Sheffield VC, Smith RJ: **Pendred syndrome, DFNB4, and PDS/SLC26A4 identification of eight novel mutation and possible genotype–phenotype correlations.** *Hum Mutat* 2001, **17**:404–411.
13. Usami S, Abe S, Weston MD, Shinkawa H, Camp GV, Kimberling WJ: **Non-syndromic hearing loss associated with enlarged vestibular aqueduct is caused by PDS mutations.** *Hum Genet* 1999, **104**:188–192.
14. Park HJ, Shaukat S, Liu XZ, Hahn SH, Naz S, Ghosh M, Kim HN, Moon SK, Abe S, Tsukamoto K, Riazuddin S, Kabra M, Erdenetungalag R, Radnaabazar J, Khan S, Pandya A, Usami S-I, Nance WE, Wilcox ER, Riazuddin S, Griffith AJ: **Origins and frequencies of SLC26A4 (PDS) mutations in east and south Asians: Global implications for the epidemiology of deafness.** *J Med Genet* 2003, **40**:242–248.
15. Tsukamoto K, Suzuki H, Harada D, Namba A, Abe S, Usami S: **Distribution and frequencies of PDS (SLC26A4) mutations in Pendred syndrome and nonsyndromic hearing loss associated with enlarged vestibular aqueduct: a unique spectrum of mutations in Japanese.** *Eur J Hum Genet* 2003, **11**:916–922.
16. Japanese Archipelago Human Population Genetics Consortium, Jinam T, Nishida N, Hirai M, Kawamura S, Oota H, Umetsu K, Kimura R, Ohashi J, Tajima A, Yamamoto T, Tanabe H, Mano S, Suto Y, Kaname T, Naritomi K, Yanagi K, Niikawa N, Omoto K, Tokunaga K, Saitou N: **The history of human populations in the Japanese Archipelago inferred from genome-wide SNP data with a special reference to the Ainu and the Ryukyuan populations.** *J Hum Genet* 2012, **57**:787–795.
17. Valvassori GE, Clemis JD: **The large vestibular aqueduct syndrome.** *Laryngoscope* 1978, **88**:723–728.
18. Phelps PD: **The basal turn of the cochlea.** *Br J Radiol* 1992, **65**:370–374.
19. Goldfeld M, Glaser B, Nassir E, Gomori JM, Hazani E, Bishara N: **CT of the ear in pendred syndrome.** *Radiology* 2005, **235**:537–540.
20. Davidson HC, Harnsberger HR, Lemmerling MM, Mancuso AA, White DK, Tong KA, Dahlen RT, Shelton C: **MR evaluation of vestibulocochlear anomalies associated with large endolymphatic duct and sac.** *AJNR Am J Neuroradiol* 1999, **20**:1435–1441.
21. Fraser GR: **Association of congenital deafness with goiter (Pendred's syndrome): a study of 207 families.** *Ann Hum Genet* 1965, **28**:201–249.
22. Valvassori GE: **The large vestibular aqueduct and associated anomalies of the inner ear.** *Otolaryngol Clin North Am* 1983, **16**:95–101.
23. Jackler RK, de la Cruz A: **The large vestibular aqueduct syndrome.** *Laryngoscope* 1989, **99**:1238–1243.
24. Levenson MJ, Parisier SC, Jacobs M, Edelstein DR: **The large vestibular aqueduct syndrome in children.** *Arch Otolaryngol Head Neck Surg* 1989, **115**:54–58.
25. Arcand P, Desrosiers M, Dube J, Abela A: **The large vestibular aqueduct syndrome and seisorineural hearing loss in the pediatric population.** *J Otolaryngol* 1991, **20**:247–250.
26. Belenky WM, Madgy DN, Leider JS, Becker C, Hotaling AJ: **The enlarged vestivular aqueduct syndrome (EVA syndrome).** *ENT J* 1993, **72**:746–751.
27. Okumura T, Takahashi H, Honjo I, Takagi A, Mitamura K: **Sensorineural hearing loss in patients with large vestibular aqueduct.** *Laryngoscope* 1995, **105**:289–294.
28. Stinckens C, Huygen PL, Joosten FB, Van Camp G, Otten B, Cremers CW: **Fluctuant, progressive hearing loss associated with Meniere like vertigo in three patients with the Pendred syndrome.** *Int J Pediatr Otorhinolaryngol* 2001, **61**:207–215.
29. Cremers CW, Admiraal RJ, Huygen PL, Bolder C, Everett LA, Joosten FB, Green ED, van Camp G, Otten BJ: **Progressive hearing loss, hypoplasia of the cochlea and widened vestibular aqueducts are very common features in Pendred's syndrome.** *Int J Pediatr Otorhinolaryngol* 1998, **45**:113–123.
30. Dossena S, Rodighiero S, Vezzoli V, Nofziger C, Salvioni E, Boccazzi M, Grabmayer E, Botta G, Meyer G, Fugazzola L, Beck-Peccoz P, Paulmichl M: **Functional characterization of wildtype and mutated pendrin (SLC26A4), the anion transporter involved in Pendred syndrome.** *J Mol Endocrinol* 2009, **43**:93–103.
31. Fugazzola L, Cerutti N, Mannavola D, Vannucchi G, Beck-Peccoz P: **The role of pendrin in iodide regulation.** *Exp Clin Endocr Diab* 2001, **109**:18–22.
32. Scott D, Wang R, Kreman T, Sheffield V, Karniski L: **The Pendred syndrome gene encodes a chloride-iodide transport protein.** *Nat Genet* 1999, **21**:440–443.
33. Scott DA, Wang R, Kreman TM, Andrews M, McDonald JM, Bishop JR, Smith RJH, Karnishki LP, Sheffield VC: **Functional differences of the PDS gene product are associated with phenotypic variation in patients with Pendred syndrome and non-syndromic hearing loss (DFNB4).** *Hum Mol Genet* 2000, **9**:1709–1715.
34. Reardon W, Coffey R, Chowdhury T, Grossman A, Jan H, Britton K, Kendall-Taylor P, Trembath R: **Prevalence, age of onset, and natural history of thyroid disease in Pendred syndrome.** *J Med Genet* 1999, **36**:595–598.
35. Napiontek U, Borck G, Muller-Forell W, Pfarr N, Bohnert A, Keilmann A, Pohlenz J: **Intrafamilial variability of the deafness and goiter phenotype in Pendred syndrome caused by a T416P mutation in the SLC26A4 gene.** *J Clin Endocrinol Metab* 2004, **89**:5347–5351.
36. Iwasaki S, Tsukamoto K, Usami S, Misawa K, Mizuta K, Mineta H: **Association of SLC26A4 mutation with clinical features and thyroid function in deaf infants with enlarged vestibular aqueduct.** *J Hum Genet* 2006, **51**:805–810.
37. Kitamura K, Takahashi K, Noguchi Y, Kuroishikawa Y, Tamagawa Y, Ishikawa K, Ichimura K, Hagiwara H: **Mutations of the Pendred syndrome gene (PDS) in patients with large vestibular aqueduct.** *Acta Otolaryngol* 2000, 120:137–141.

38. Dai P, Li Q, Huang D, Yuan Y, Kang D, Miller DT, Shao H, Zhu Q, He J, Yu F, Liu X, Han B, Yuan H, Platt OS, Han D, Wu BL: **SLC26A4 c.919-2A > G varies among Chinese ethnic groups as a cause of hearing loss.** *Genet Med* 2008, **10**:586–592.
39. Chen K, Wang X, Sun L, Jiang H: **Screening of SLC26A4, FOXI1, KCNJ10, and GJB2 in bilateral deafness patients with inner ear malformation.** *Otolaryngol Head Neck Surg* 2012, **146**:972–978.
40. Wu CC, Yeh TH, Chen PJ, Hsu CJ: **Prevalent SLC26A4 mutations in patients with enlarged vestibular aqueduct and/or Mondini dysplasia: a unique spectrum of mutations in Taiwan, including a frequent founder mutation.** *Laryngoscope* 2005, **115**:1060–1064.
41. Shin JW, Lee SC, Lee HK, Park HJ: **Genetic screenig of GJB2 and SLC26A4 in Korean cochlear implantees: experience of soree Ear clinic.** *Clin Exp Otorhinolaryngol* 2012, **30**(Suppl 1):10–13.
42. Yang JJ, Tsai CC, Hsu HM, Shiao JY, Su CC, Li SY: **Hearing loss associated with enlarged vestibular aqueduct and Mondini dysplasia is caused by splice-site mutation in the PDS gene.** *Hear Res* 2005, **199**:22–30.
43. Wang QJ, Zhao YL, Rao SQ, Guo YF, Yuan H, Zong L, Guan J, Xu BC, Wang DY, Han MK, Lan L, Zhai SQ, Shen Y: **A distinct spectrum of SLC26A4 mutations in patients with enlarged vestibular aqueduct in China.** *Clin Genet* 2007, **72**:245–254.
44. Reyes S, Wang G, Ouyang X, Han B, Du LL, Yuan HJ, Yan D, Dai P, Liu XZ: **Mutation analysis of SLC26A4 in mainland Chinese patients with enlarged vestibular aqueduct.** *Otolaryngol Head Neck Surg* 2009, **141**:502–508.
45. Huang S, Han D, Yuan Y, Wang G, Kang D, Zhang X, Yan X, Meng X, Dong M, Dai P: **Extremely discrepant mutation spectrum of SLC26A4 between Chinese patients with isolated Mondini deformity and enlarged vestibular aqueduct.** *J Transl Med* 2011, **30**:167.
46. Krawczak M, Reiss J, Cooper DN: **The mutational spectrum of single base-pair substitutions in mRNA splice junctions of human genes: causes and consequences.** *Hum Genet* 1992, **90**:41–54.
47. Larriba S, Bassas L, Gimenez J, Ramos MD, Segura A, Nunes V, Estivill X, Casals T: **Testicular CFTR splice variants in patients with congenital absence of the vas deferens.** *Hum Mol Genet* 1998, **7**:1739–1744.
48. Betsalel OT, Rosenberg EH, Almeida LS, Kleefstra T, Schwartz CE, Valayannopoulos V, Abdul-Rahman O, Poplawski N, Vilarinho L, Wolf P, den Dunnen JT, Jakobs C, Salomons GS: **Characterization of novel SLC6A8 variants with the use of splice-site analysis tools and implementation of a newly developed LOVD database.** *Eur J Hum Genet* 2011, **19**:56–63.

doi:10.1186/1471-2350-14-56
Cite this article as: Ganaha *et al.*: Pathogenic substitution of IVS15 + 5G > A in *SLC26A4* in patients of Okinawa Islands with enlarged vestibular aqueduct syndrome or Pendred syndrome. *BMC Medical Genetics* 2013 14:56.

ORL

ORL 2013;75:342–349
DOI: 10.1159/000357474
Received: November 23, 2012
Accepted after revision: November 18, 2013
Published online: January 10, 2014

0301–1569/14/0756–0342$39.50/0
www.karger.com/orl

Original Paper

Glucose Metabolism in the Primary Auditory Cortex of Postlingually Deaf Patients: An FDG-PET Study

Takumi Okuda[a] Shigeki Nagamachi[b] Yasuaki Ushisako[a] Tetsuya Tono[a]

Departments of [a]Otolaryngology – Head and Neck Surgery and [b]Nuclear Medicine, Miyazaki University School of Medicine, Miyazaki, Japan

Key Words
FDG-PET · Neuroplasticity · Auditory cortex · Deafness

Abstract
Background/Purpose: Previous FDG-PET studies have indicated neuroplasticity in the adult auditory cortex in cases of postlingual deafness. In the mature brain, auditory deprivation decreased neuronal activity in primary auditory and auditory-related cortices. In order to re-evaluate these issues, we used statistical analytic software, namely a three-dimensional stereotaxic region of interest template (3DSRT), in addition to statistical parametric mapping (SPM; Institute of Neurology, University College of London, UK). ***Materials and Methods:*** ^{18}F-FDG brain PET scans were performed on 7 postlingually deaf patients and 10 healthy volunteers. Significant increases and decreases of regional cerebral glucose metabolism in the patient group were estimated by comparing their PET images with those of healthy volunteers using SPM analysis and 3DSRT. ***Results:*** SPM revealed that the glucose metabolism of the deaf patients was lower in the right superior temporal gyrus, both middle temporal gyri, left inferior temporal gyrus, right inferior lobulus parietalis, right posterior cingulate gyrus, and left insular cortex than that of the control subjects. 3DSRT data also revealed significantly decreased glucose metabolism in both primary auditory cortices of the postlingually deaf patients. ***Conclusion:*** SPM and 3DSRT analyses indicated that glucose metabolism decreased in the primary auditory cortex of the postlingually deaf patients. The previous results of PET studies were confirmed, and our method involving 3DSRT has proved to be useful.

Takumi Okuda
Department of Otolaryngology – Head and Neck Surgery
Miyazaki University School of Medicine
Kiyotakecho Kihara 5200, Miyazaki, Miyazaki 889-1692 (Japan)
E-Mail takumi_okuda@med.miyazaki-u.ac.jp

ORL 2013;75:342–349
DOI: 10.1159/000357474

Introduction

Previous FDG-PET studies have indicated neuroplasticity in the adult auditory cortex in cases of postlingual deafness. In the early 1990s, this phenomenon was discussed based on visual findings. In PET images, different colors indicate different rates of glucose metabolism. That is, red indicates a high rate, yellow a moderate, and blue a low rate [1]. Patient and normal control groups were compared in this way. Then, in the 2000s, a similar comparison was performed using voxel-based analysis software such as statistical parametric mapping (SPM; Institute of Neurology, University College of London, UK) [2]. SPM has been widely used for the objective analysis of brain images. This software package compares the differences between two anatomically standardized groups with the linear model at each voxel. However, it is sometimes not possible to detect slight differences because of technical issues. In the mature brain, auditory deprivation decreases neuronal activity transiently in the primary auditory and auditory-related cortices. In order to reevaluate these issues, we used a further statistical analytic software, namely a three-dimensional stereotaxic region of interest (ROI) template (3DSRT) [3], in addition to SPM. 3DSRT is fully automated ROI-based analysis software for the brain. It was established to perform ROI analysis of the brain with improved objectivity and excellent reproducibility [4–7].

Materials and Methods

In a resting state (eyes closed, ears unoccluded, dark and quiet environment), 185-MBq ^{18}F-FDG (the dose was adjusted according to the body weight of each subject) brain PET scans were performed on 7 postlingually deaf patients and 10 healthy volunteers using the Biograph 16 PET scanner (Siemens). Seven patients (2 men, 5 women; mean age, 55.7 ± 8.7 years) underwent FDG-PET scans at Miyazaki University Hospital between July 2012 and August 2013. The duration of deafness ranged from 1 to 30 years (mean duration, 13.4 ± 10.8). The clinical features of the patients are listed in table 1. They had neither cerebral disease nor visual disturbance. Ten age-matched healthy volunteers (2 men, 8 women; mean age, 57.9 ± 16.2 years) served as control subjects. Exclusion criteria for the control subjects included a history of any neurological, psychiatric or significant medical illness, or a history of drug abuse. All patients and control subjects were right-handed. Detailed explanations of the procedure, risk, and purpose of the FDG-PET study were provided to them. The present work was approved by the Ethics Committee of Miyazaki University School of Medicine, and written consent was obtained from each participant.

Significant increases and decreases of regional cerebral glucose metabolism in the patient group were estimated by comparing their FDG-PET images with those of the healthy volunteers using SPM analysis.

We also compared the glucose metabolism of auditory cortices with that of visual cortices using 3DSRT. Because all patients and control subjects had neither cerebral disease nor visual disturbances, we adopted the primary visual cortex as a reference. 3DSRT applies constant ROIs on anatomically standardized images and enables image analysis of miscellaneous radioactive tracers (^{99m}Tc-ECD, ^{123}I-IMP, [^{15}O]-H_2O, and ^{18}F-FDG) with excellent reproducibility and objectivity. The analytical process of this method is as follows: (1) anatomical standardization using the SPM algorithm; (2) analysis using 318 constant ROIs divided into 12 groups (segments) on each hemisphere; (3) calculation of the area-weighted average for each of the respective 24 segments based on the value in each ROI, and (4) display of the results followed by saving of the respective values of the 636 ROIs (both hemispheres) in the CSV file format. For 3DSRT analysis, 318 constant ROIs on each brain hemisphere were prepared. The constant ROIs were determined on the T1-weighted magnetic resonance images (MRI) anatomically standardized by SPM and classified into 12 segments according to their arterial supply. 3DSRT allows for quantitative analysis, in contrast to SPM, which involves statistical analysis.

Table 1. Clinical features of deaf patients

Patient No.	Age, years	Sex	Cause of deafness	Duration of deafness, years
1	50	F	Unknown	1
2	52	F	Unknown	24
3	63	F	Unknown	1
4	49	F	Head injury	30
5	47	M	Otosclerosis	13
6	72	M	Unknown	5
7	57	F	Unknown	20

Table 2. Significantly decreased glucose metabolism (deaf versus normal)

Region	Coordinates*			Analysis	
	x	y	z	Z**	p
Right middle temporal gyrus	43.6	−12.1	−8.6	3.67	0.001
Right inferior lobulus parietalis	23.8	−38.9	40.0	3.61	0.002
Right superior temporal gyrus	39.6	−2.2	−5.4	3.44	0.002
Right posterior cingulate gyrus	23.8	−39.1	37.0	3.61	0.003
Right posterior cingulate gyrus	23.8	−23.4	38.0	3.41	0.035
Left middle temporal gyrus	−41.6	−25.5	−4.3	3.35	0.008
Left inferior temporal gyrus	−35.6	−3.0	−20.1	3.29	0.009
Left insular cortex	−39.6	3.8	−2.03	3.09	0.011

* International Consortium on Brain Mapping coordinates for the location where the significant difference between conditions was centered.

** Z values refer to the comparison of normalized glucose metabolism between the deaf and the normal group.

Results

When we compared the ^{18}F-FDG brain PET images of the postlingually deaf patients with those of the healthy control subjects (fig. 1) by using the SPM method, the glucose metabolism of the deaf patients was lower in the right superior temporal gyrus, both middle temporal gyri, left inferior temporal gyrus, right inferior lobulus parietalis, right posterior cingulate gyrus, and left insular cortex (table 2). The 3DSRT data also revealed significantly decreased glucose metabolism in both primary auditory cortices of the postlingually deaf patients. We found a 13% decrease in the right hemisphere and a 16% decrease in the left hemisphere (fig. 2).

Discussion

Generally, cortical glucose metabolism in the sensory system characteristically decreases with sensory deficits, owing to the absence of central sensory input. The same pattern has been observed in the auditory system [8].

In the early 1990s, glucose metabolism in the auditory cortices was compared by PET on a visual basis. In PET images, different colors indicate different rates of glucose metabolism. That is, red indicates a high rate, yellow a moderate, and blue a low rate [1]. Since the early 2000s, SPM has been used for these studies [2]. Voxel-based analysis software such as SPM

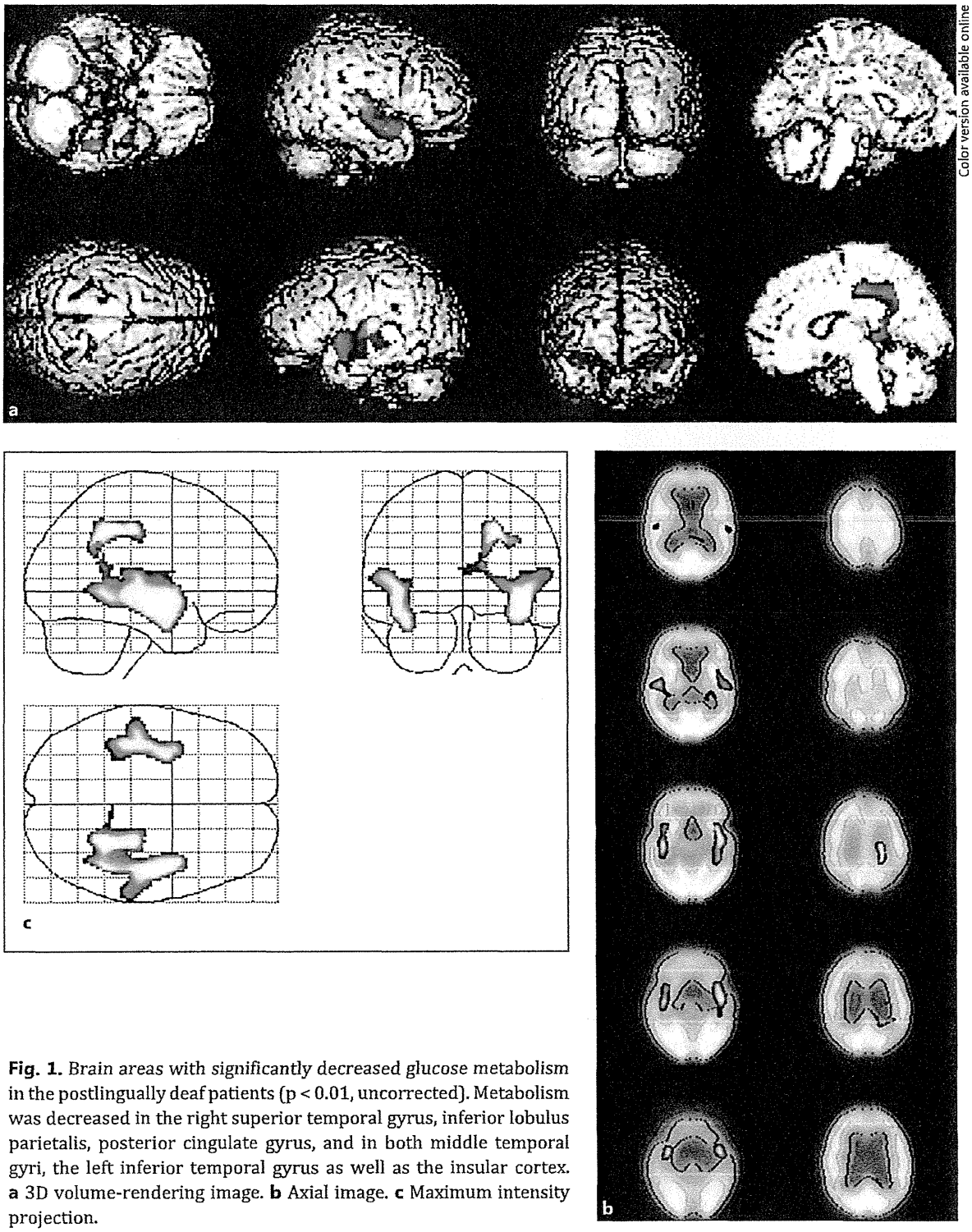

Fig. 1. Brain areas with significantly decreased glucose metabolism in the postlingually deaf patients ($p < 0.01$, uncorrected). Metabolism was decreased in the right superior temporal gyrus, inferior lobulus parietalis, posterior cingulate gyrus, and in both middle temporal gyri, the left inferior temporal gyrus as well as the insular cortex. **a** 3D volume-rendering image. **b** Axial image. **c** Maximum intensity projection.

ORL 2013;75:342–349
DOI: 10.1159/000357474

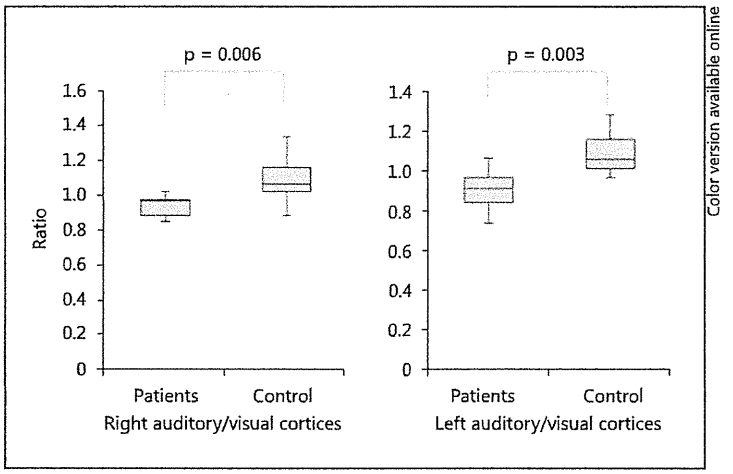

Fig. 2. 3DSRT data revealed significantly decreased glucose metabolism in both primary auditory cortices of the postlingually deaf patients.

has been widely used for the objective analysis of brain images with various imaging drugs. There are several reports about changes in the glucose uptake in the auditory cortex observed by FDG-PET.

In prelingually deaf children, the hypometabolic area of the auditory cortex was widest initially, but decreased as the duration of deafness increased. After 20 years of deafness, cortical glucose metabolism did not differ from that of normal controls [9]. This finding was supported by animal studies. In neonatal deafened rats, the same pattern was observed [10]. In addition, Lee et al. [9] found a positive correlation between the hearing performance of prelingually deafened children after cochlear implantation and the extent of the preoperative hypometabolic area in the auditory cortex. Glucose metabolism in the temporal lobe of deaf children increases with age, and the hearing outcomes deteriorate accordingly. We consider that this phenomenon involves the cross-modal plasticity of the brain. Because of the long-term absence of auditory input in congenitally deaf children, the auditory cortex is gradually displaced for another sensory center. Therefore, as the child grows older and the duration of deafness increases, the hearing-capability score with a cochlear implant gets worse. An FDG-PET study before cochlear implantation can predict the prognosis for prelingually deaf children.

Indeed, there are some reports of visual language activation studies by FDG-PET describing that the auditory association area of a deaf child develops to process visual aspects of language if it does not receive sufficient auditory signals in the developmental period. In addition, this cross-modal plasticity is suppressed and replaced by normal development if the child uses a hearing prosthesis such as a hearing aid or a cochlear implant to increase his or her spoken language skills [11, 12].

This fact was confirmed by other methods such as magnetoencephalography or functional MRI. Levänen et al. [13] reported that vibrotactile stimuli, applied on the palm and fingers of a congenitally deaf adult, activated his/her auditory cortices. The recorded magnetoencephalography signals also indicated that the auditory cortices could discriminate between the applied 180- and 250-Hz vibration frequencies. Similar to the visual language activation study by FDG-PET, these findings suggest that human cortical areas, normally subserving hearing, may process vibrotactile information in the congenitally deaf because of the lack of auditory signals. Sadato et al. [14] used functional MRI to study prelingually deaf signers, hearing non-signers, and hearing signers. The visually presented tasks included mouth-movement matching, random-dot motion matching, and sign-related motion matching.